Libraries and Learning Services

University of Auckland Research Repository, ResearchSpace

Version

This is the Accepted Manuscript version. This version is defined in the NISO recommended practice RP-8-2008 http://www.niso.org/publications/rp/

Suggested Reference

Lumantarna, R., Biggs, D. T., & Ingham, J. M. (2014). Uniaxial Compressive Strength and Stiffness of Field-Extracted and Laboratory-Constructed Masonry Prisms. *Journal of Materials in Civil Engineering*, *26*(4), 567-575. doi:10.1061/(ASCE)MT.1943-5533.0000731

Copyright

Items in ResearchSpace are protected by copyright, with all rights reserved, unless otherwise indicated. Previously published items are made available in accordance with the copyright policy of the publisher.

For more information, see General copyright, Publisher copyright, SHERPA/RoMEO.

Manuscript
Click here to download Manuscript: Uniaxial compressive strength and stiffness of field extracted and laboratory constructed masonry pris

Title: Uniaxial compressive strength and stiffness of field extracted and laboratory constructed masonry prisms

Ronald Lumantarna[1], David T. Biggs[2] Dist.M. ASCE and Jason M. Ingham[3] M. ASCE

ABSTRACT

Masonry material characteristics such as compression stress-strain behaviour and the relationships between brick, mortar and masonry compressive strengths are required for the detailed analysis and assessment of masonry structures. These properties have been investigated previously, but most past studies were laboratory based and did not include within their scope the testing of existing masonry buildings. The present study aimed to characterise the compressive strength and the compression stress-strain relationship of vintage clay brick masonry used in New Zealand unreinforced masonry (URM) bearing wall buildings that were generally constructed between 1880 and 1940. Testing was performed on 45 masonry prisms that were extracted from eight New Zealand historic URM buildings and on 75 masonry prisms that were constructed in the laboratory using 14 different brick/mortar combinations. It was found that the laboratory constructed sample test results adequately replicated those from the field extracted samples, and predictive equations and a numerical compression stress-strain model for use in the detailed seismic assessment of URM buildings were developed based on the experimental results.

[1] Ph.D. student, Department of Civil & Environmental Engineering, University of Auckland, Private Bag 92019, Auckland 1010, New Zealand, rlum009@aucklanduni.ac.nz
[2] Principal, Biggs Consulting Engineering, Troy, New York 12180-6671, USA, biggsconsulting@att.net
[3] Associate Professor, Department of Civil & Environmental Engineering, University of Auckland, Private Bag 92019, Auckland 1010, New Zealand, j.ingham@auckland.ac.nz

CE Database subject headings: Brick; Mortar; Masonry; Compressive strength; Stiffness; Modulus of Elasticity; Strain

INTRODUCTION

An unreinforced masonry (URM) assemblage is a non-homogeneous, inelastic and orthotropic material constructed using individual brick units and mortar, and therefore the properties of the assemblage are influenced by both the brick unit and the mortar properties. Masonry assemblage properties, such as the masonry constitutive relationship and Modulus of Elasticity, are required for linear and non-linear analyses of masonry structures (Kaushik et al. 2007a; Kaushik et al. 2007b). Masonry compression stress-strain characteristics and the relationships between masonry compressive strength and the constituent material properties have been investigated by past researchers (Deodhar 2000; Gumaste et al. 2006; Kaushik et al. 2007a; Kaushik et al. 2007b). However, most of these past studies were laboratory based and did not include within their scope the testing of samples extracted from existing masonry buildings.

The work presented here was undertaken to investigate the compressive strength and the compression stress-strain characteristics of New Zealand URM bearing wall buildings that were generally constructed between 1880 and 1940 (Russell and Ingham 2010). 45 masonry prisms were extracted from 8 existing New Zealand URM buildings, and 75 prisms having 14 different brick/mortar combinations were constructed for comparison using New Zealand vintage solid clay bricks and a range of mortar strengths. These extracted and laboratory constructed prisms were laboratory tested, and predictive expressions relating masonry compressive strength to the constituent material compressive strengths and to the masonry Modulus of Elasticity were developed based on the experimental results. Masonry compression stress-strain numerical

models were also developed to enable the prediction of masonry stress-strain behaviour. Whilst noting that the variability of aged masonry made the development of precise relationships unrealistic, the primary objective of this study was to develop predictive expressions that are sufficiently accurate to use in the detailed seismic assessment of regular URM bearing wall buildings.

PAST STUDIES ON MASONRY COMPRESSIVE PROPERTIES

Relationship between brick, mortar and masonry compressive strength

Masonry compressive strength is one of the most important properties for the assessment and design of masonry elements (Kaushik et al. 2007a). However, compression testing of masonry prisms is not always practical, and therefore many researchers (Deodhar 2000; Gumaste et al. 2006; Kaushik et al. 2007a; Kaushik et al. 2007b) have attempted to develop an empirical expression relating the brick unit, mortar and masonry compressive strengths in a form such as shown in Equation 1 (CEN 2005)

$$f'_m = K f'^{\alpha}_b \times f'^{\beta}_j \quad (1)$$

where K, α and β are constants, and f'_b , f'_j and f'_m are the brick unit, mortar and masonry compressive strengths respectively. Eurocode 6 (CEN 2005) recommends a range of K values, depending on the brick unit properties and the brick/mortar bond configuration, while prescribing α and β as 0.7 and 0.3 respectively. The value of β is lower than α, which indicates that the masonry compressive strength (f'_m) is influenced to a greater extent by the brick unit compressive strength (f'_b) than by the mortar compressive strength (f'_j). It is noted that the

constants proposed by Eurocode 6 (CEN 2005) are used to estimate the 5% lower characteristic compressive strength of masonry, instead of the mean compressive strength.

Kaushik et al. (2007a) conducted experiments using four different brick unit types and three different mortar grades, adopted the Eurocode 6 expression (Equation 1) and found that using mean material compressive strengths, K, α and β were equal to 0.63, 0.49 and 0.32. In addition, Gumaste et al. (2006) found that using mean material compressive strengths, K, α and β were equal to 0.32, 0.87 and 0.13 for stack bonded prisms that were constructed using two different brick types and five different mortar mixes, which indicated that the mortar compressive strength had little influence on the masonry compressive strength.

Relationship between masonry compressive strength and Modulus of Elasticity

The masonry Modulus of Elasticity (E_m) is commonly calculated as the chord modulus of the linear part of the masonry compression stress-strain curve, which is typically defined to be between 5% and 33% of the ultimate masonry compressive strength (f'_m) (ASTM 2003a; Drysdale et al. 1999). Alternatively, Gumaste et al. (2006) used the secant modulus at $0.25f'_m$ to calculate the masonry Modulus of Elasticity. The relationship between masonry compressive strength and Modulus of Elasticity can be expressed as

$$E_m = k\, f'_m \qquad (2)$$

where k is a constant that varies from one recommendation to another. The MSJC code (2002) and FEMA 306 (1999) from North America recommend that E_m is equal to $700f'_m$ for modern masonry and $550f'_m$ for existing masonry respectively, whilst the Canadian masonry code (CSA 2004) suggests a slightly higher value of $E_m = 850f'_m$ for modern masonry. Paulay and Priestley (1992) and Eurocode 6 (CEN 2005) suggest that E_m is equal to $750f'_m$ and $1000f'_m$ respectively.

In addition, Kaushik et al. (2007a) observed that there was a wide variation in the Modulus of Elasticity-compressive strength relationships of newly constructed Indian clay brick masonry, where the E_m values varied from $250f'_m$ to $1100f'_m$. This wide variation was also observed by Drysdale et al. (1999), who collected past experimental data and encountered E_m values ranging from $210f'_m$ to $1670f'_m$.

Numerical masonry compression stress-strain model

Knowledge of masonry compression stress-strain behaviour is important for accurate non-linear structural analysis (Kaushik et al. 2007b). In addition, masonry stress-strain characteristics influence masonry deformation modes, and therefore accurate characterisation of masonry compression stress-strain behaviour is essential to study masonry structural performance characteristics that are material dependent, such as the in-plane seismic response of unreinforced masonry piers. Priestley and Elder (1983) introduced the "modified" Kent-Park model to characterise the compression stress-strain behaviour of concrete masonry. This model incorporates a parabolic ascending stress-strain curve, followed by a linear descending part and a horizontal plateau at 20% of masonry compressive strength.

Seible and Kingsley (1991) proposed a principal compression stress-strain law for unconfined masonry in compression. This model incorporates a parabolic stress-strain curve which extends until 160% of the strain at f'_m, followed by an exponential descending part and a horizontal plateau at 10% of masonry compressive strength. Kaushik et al. (2007a) adopted the model developed by Kent and Park (1971), which was intended for confined concrete having steel hoops or spirals, and rearranged the expression as per Equation 3:

$$\frac{f_m}{f'_m} = 2\frac{\varepsilon_m}{\varepsilon'_m} - \left(\frac{\varepsilon_m}{\varepsilon'_m}\right)^2 \quad (3)$$

where f_m and ε_m = masonry stress and strain respectively; and ε'_m = masonry strain corresponding to f'_m. Kaushik et al. (2007a) found that this parabolic stress-strain model matched their experimental stress-strain curves until the peak stress was reached. The immediate post-peak compression stress-strain behaviour descending to $0.9f'_m$ was also represented using Equation 3, followed by a linear descending part and a horizontal plateau at $0.2f'_m$. Two possible linear descending parts were proposed whilst considering the ductility provided by lime mortar: a straight line connecting the stress-strain curve between $0.9f'_m$ and $2.75\varepsilon'_m$ for prisms constructed using cement-lime mortar, and a straight line between $0.9f'_m$ and $2\varepsilon'_m$ for prisms constructed using mortar without lime. Kaushik et al. (2007a) suggested that the masonry strain at peak strength (ε'_m) can be estimated as per Equation 4, where a, b and c are constants of 0.27, 0.25 and 0.7 respectively.

$$\varepsilon'_m = \frac{af'_m}{{f'_j}^b {E_m}^c} \quad (4)$$

EXPERIMENTAL PROGRAMME

The experimental programme involved the compression testing of both field extracted and laboratory constructed masonry prisms. 45 masonry prisms extracted from eight historic New Zealand URM bearing wall buildings were either cut in-situ using a masonry chainsaw or were extracted as irregular masonry segments. These samples were further trimmed in the laboratory to form single leaf three brick high prisms (see Figure 1). Plastering and rendering mortars were removed, if present. Three brick high prisms were selected for ease of sample handling. The cutting process and the transportation of samples from their source to the testing laboratory were performed carefully in order to minimise disturbance to the mortar joints. There were rare

127 occasions when the mortar joint of a sample was broken during the cutting process. However,
128 these broken samples were discarded, and all retained samples were those that remained intact
129 and were largely undisturbed throughout the sample preparation process.
130 75 three brick high masonry prisms having 14 different brick/mortar combinations were prepared
131 with occasional assistance provided by an experienced mason, and were left to cure for at least
132 28 days at room temperature (20 ± 5º C) before testing. The masonry units used in these
133 constructed prisms were recycled vintage solid clay bricks obtained from demolition contractors,
134 with an average $l \times w \times h$ of 228 mm × 112 mm × 78 mm, and the thickness of the mortar joints
135 was maintained between 12 mm and 18 mm to replicate common New Zealand URM
136 construction practice.
137 Preliminary laboratory experiments revealed that the brick/mortar bond was poor when dry brick
138 units were used, and therefore the brick units used in the experimental programme were first
139 submerged in water for ten minutes before laying, following the procedure reported by
140 Sarangapani et al. (2005), to accommodate brick/mortar bond development.
141 All prisms were capped using gypsum plaster and tested in compression following ASTM
142 C 1314 - 03b (2003a) using a 2000 kN Instron machine (see Figure 2). For most tests, two
143 laboratory-calibrated displacement gauges were attached on the left and right sides of the prisms,
144 spanning from the middle of the bottom brick to the middle of the top brick, thus enabling the
145 masonry compression stress-strain relationship and Modulus of Elasticity to be derived. The
146 stress and displacement values were recorded using data acquisition software, and the strain was
147 calculated using the average readings from the two displacement gauges.
148 ASTM C 1314 - 03b (2003a) recommends that masonry prisms used for compression testing be
149 at least two bricks high whilst having a height to thickness ratio between 1.3 and 5.0, and

correction factors are provided in ASTM C 1314 - 03b (2003a) according to the sample height to thickness (*h/t*) ratio to account for the influence of varying sample dimensions. Kingsley and Noland (1992) reported that a decrease in sample *h/t* ratio led to an increase in the measured prism compressive strength as the top and bottom loading platens introduced confining stresses that affected the measured values. Furthermore, Morel et al. (2007) described that these confining stresses occurred due to friction between the loading platens and the test specimen, and that the confinement effect decreased as the distance between the loading platens increased. Considering the above factors, all prisms used in this experimental programme were three brick high prisms to maintain consistency in the analysis, and *h/t* ratio correction factors as prescribed in ASTM C 1314 - 03b (2003a) were incorporated.

Constituent masonry material properties

The compressive strength of the brick units that were used in each prism combination was determined following the half brick compression test ASTM C 67 - 03a (2003b). Irregular mortar samples were extracted from each field site and carefully cut in the laboratory to form rectangular test pieces, then capped using gypsum plaster and tested in compression following the procedure reported by Lumantarna (2012). ASTM C 67 - 03a (2003b) prescribes the use of half brick units for compression testing, to reduce the confinement effects introduced by the loading platens, and the irregular mortar compression test procedure prescribed in Lumantarna (2012) accounts for the specimen aspect ratio and footprint dimensions as these factors clearly influence the measured mortar compressive strength.

For the laboratory constructed prisms, varying mortar mix proportions were selected to simulate a wide range of mortar properties, and the materials used in the mortar were ordinary Portland

cement, hydrated lime and river sand. Most of the mortar mix proportions chosen were based on the proportions recommended in ASTM C 270 - 08a (2008a) and on the typical material proportions for New Zealand historic mortar as reported in NZSEE (2006), except for mortar grades B and E, which were approximated by the mason that assisted in the sample construction process. The water:cement ratio of each mortar grade was kept constant to maintain between-batch consistency. It is noted that these mortar cubes were prepared simultaneously with the laboratory constructed prisms. The compressive strength of each mortar grade was determined using 50 mm mortar cubes that were prepared as prescribed in ASTM C 109 - 08 (2008b). After approximately 28 days of curing at room temperature (20 ± 5º C), these mortar cubes were tested in compression following ASTM C 109 - 08 (2008b).

Table 1 and

183 Table 2 present the constituent material properties of the field extracted and the laboratory
184 constructed prisms respectively, where n is the number of samples tested. The origin and the year
185 of construction of the field extracted prisms are also reported in Table 1. It is noted that some of
186 the brick groups used to construct the laboratory prisms reported in

187 Table 2 were recycled from the field sites shown in Table 1, and thus the designations for the
188 brick groups as listed in

Table 2 were kept consistent with the field site designations reported in Table 1.

The brick unit and mortar compressive strengths varied from 8.5 MPa to 43.4 MPa and from 0.69 MPa to 23.2 MPa respectively. In general, the coefficients of variation (CoV) of the brick units were greater than those of the mortar, where the CoV ranged from 0.15 to 0.28 for the brick units and from 0.04 to 0.26 for the mortar. Mortar grades F and G were both ASTM type N mortars, but their mean compressive strengths were different from each other. This difference in mortar compressive strength was possibly due to variation in the water:cement ratio, although this supposition could not be investigated as the water proportions for mortar grade G were not recorded. It is also noted that the mortars which had mean f'_j above 5 MPa were cement rich lime-cement mortars (the volumetric ratio of cement/lime was ≥ 1.0).

Masonry compression test results

The mean compressive strengths (f'_m), mean Modulus of Elasticity (E_m) and mean strain at peak stress (ε'_m) of the field extracted and laboratory constructed prisms are presented in

202 Table 3. 75 prisms were laboratory constructed using the eight different brick groups and eight
203 different mortar grades. The preparation of compression tests that incorporated displacement
204 gauges was found to be time consuming, and thus some prisms were not compression tested
205 incorporating displacement gauges. The n and n* values shown in

206 Table 3 are the number of test results included in the mean f'_m and mean f'_m* calculations
207 respectively.

Table 3 provides two different f'_m values for each prism combination, as not all prisms were tested incorporating displacement gauges, and therefore the mean f'_m values that correspond to the E_m and ε'_m values (referred to as f'_m*) were different to the mean f'_m values of all prisms tested. The mean f'_m values were used to develop the relationships between f'_b , f'_j and f'_m, whilst the f'_m* values were used to study the relationships between E_m, ε'_m and f'_m.

Figure 3 shows the normalised, dimensionless stress-strain relationships of the tested masonry prisms with respect to the maximum compressive stress (f'_m) and masonry strain at peak stress (ε'_m). The Young's Modulus of Elasticity is used to describe the material stress-strain behaviour if the strain of the material is linearly proportional to the applied stress within the elastic range, as described in ASTM E 111 - 97 (1997). However, Figure 3 shows that the stress-strain relationships of the samples included in this experimental programme did not exhibit a distinct linear relationship and became increasingly nonlinear for compression stresses in excess of $0.50f'_m$. Therefore, in alignment with ASTM C 1314 - 03b (2003a), it was decided that the chord Modulus of Elasticity be used to describe the stress-strain behaviour of masonry prisms included in this experimental programme.

The objective of this study was to provide information that was suitable for use in non-linear seismic analysis. As the initiation of visible damage in the tested prisms generally occurred at approximately $0.70f'_m$, it was decided that the masonry Modulus of Elasticity be calculated as the chord modulus of the stress-strain curve between $0.05f'_m$ and $0.70f'_m$ in order to provide a suitable stiffness value for use to determine effective yield displacements (Marcari et al. 2007; OPCM 2005) (see Figure 3). The readings below $0.05f'_m$ were excluded from the analysis as they were potentially influenced by initial confinement of the sample and were typically erratic. The measurement of E_m based on the stress-strain ordinates at $0.05f'_m$ and $0.33f'_m$ (as

231 recommended in ASTM C 1314 - 03b (2003a)) was deemed to potentially result in an
232 overestimation of masonry Modulus of Elasticity due to nonlinearity in the stress-strain
233 relationship.
234

Table 3 shows that the mean f'_m of the field extracted and laboratory constructed samples varied from 3.31 MPa to 30.79 MPa (CoV ranging between 0.12 and 0.25). In agreement with previous studies (Aryana and Matthys 2008; Hendry 1998; Lenczner 1972), most of the mean masonry compressive strengths were between those of the brick units and the mortar.

The mean f'_m values of the laboratory constructed samples adequately replicated those of the field extracted samples, although the extracted sample compressive strengths were mostly within the lower half of the compressive strength database. Similarly, the mean Modulus of Elasticity and mean strain at peak stress of the laboratory constructed samples satisfactorily replicated the corresponding properties of the field extracted samples (mean E_m ranged from 388 MPa to 7,971 MPa and mean ε'_m ranged from 0.0028 to 0.0143). The masonry Modulus of Elasticity and strain at peak stress were generally more variable (CoV E_m ranging from 0.11 to 0.43 and CoV ε'_m ranging between 0.07 and 0.39) than was the masonry compressive strength. When expressed in terms of mean f'_m, the mean masonry Modulus of Elasticity varied from $89f'_m$ to $433f'_m$.

It is noted that all of the field extracted masonry prisms had at least one vertical mortar head joint within their brick courses. The test results revealed that the constitutive relationships of the laboratory constructed samples aligned well with those of the field extracted samples, and therefore it was concluded that the presence of the vertical mortar head joints had minimal influence on the masonry compressive properties.

ANALYSIS AND DISCUSSION

Prediction of masonry compressive strength

An expression relating the brick unit, mortar and prism compressive strengths was derived to enable prediction of the compressive strength of existing New Zealand URM bearing wall buildings using only the brick unit and mortar compressive strengths, so that the required number of expensive and time consuming prism compression tests can be minimised.

Table 3 shows that in general, the mean masonry compressive strength increased with increasing mean brick unit and mean mortar compressive strengths. The field extracted sample test results were combined with those of the laboratory constructed samples, and a non-linear regression analysis was performed to determine the relationships between f'_b, f'_j and f'_m for the combined data set, allowing the resemblance of the laboratory constructed samples to the field extracted samples to be assessed. A three dimensional plot relating f'_b, f'_j and f'_m of the combined database was generated using DataFit 9.0 (Oakdale Engineering 2010) as illustrated in Figure 4. It was shown that the f'_b, f'_j and f'_m relationships of the laboratory constructed samples converged with those of the field extracted samples (white dots in Figure 4). The surface plot in Figure 4 represents the prediction of mean masonry compressive strength for different brick unit and mortar mean compressive strengths. A predictive equation relating f'_b, f'_j and f'_m in the form of the Eurocode 6 expression (CEN 2005) was derived, and constants K, α and β were found to be 0.75, 0.75 and 0.31 respectively (see Equation 5).

$$f'_m = 0.75 f'^{0.75}_b \times f'^{0.31}_j \quad (5)$$

In agreement with previous studies (Gumaste et al. 2006; Kaushik et al. 2007a), the β value (0.31) was found to be lower than the α value (0.75), which implied that the mean mortar compressive strength had less influence on the mean masonry compressive strength than did the mean brick unit compressive strength. Equation 5 had a coefficient of determination (R^2) value of 87%, which was deemed to be satisfactory, especially when considering that this equation suited both field extracted and laboratory constructed masonry.

Prediction of masonry Modulus of Elasticity

As masonry Modulus of Elasticity is an important property for linear and non-linear structural analysis, a predictive expression relating the masonry Modulus of Elasticity to the masonry compressive strength was derived.

Table 3 shows that the masonry Modulus of Elasticity generally increased with increasing masonry compressive strength. The masonry Modulus of Elasticity-compressive strength relationship of the combined dataset for both the field extracted and the laboratory constructed prisms is illustrated in Figure 5, showing good agreement between the two separate data sets. For the combined dataset, E_m could be satisfactorily equated to $294f'_m$. This expression had an R^2 value of 76%, which was deemed to predict the masonry Modulus of Elasticity satisfactorily. When compared with the k values recommended elsewhere, which were mostly suited for modern masonry, the derived k value of 294 for New Zealand historic clay brick masonry was notably low, although this derived value was within the range observed by Drysdale et al. (1999) and Kaushik et al. (2007a). Another reason for the derived k value being lower than is customarily recommended was that the masonry Modulus of Elasticity was calculated using the stress and strain ordinates at $0.05f'_m$ and $0.70f'_m$ instead of those located at $0.05f'_m$ and $0.33f'_m$ as used by previous researchers. This adopted calculation method generated a linear stiffness value appropriately reflecting the measured non-linear behaviour for the strain range up to ε'_m, and therefore although the derived E_m values were low, they were thought to be representative for use in both linear and non-linear seismic analyses.

Prediction of masonry strain at peak stress

The masonry strain at peak stress is required for numerical modelling of the masonry compression stress-strain curve (refer to Equation 3), and therefore an expression was sought to predict ε'_m. Kaushik et al. (2007a) proposed that ε'_m be predicted using a function that involved masonry compressive strength, mortar compressive strength and masonry Modulus of Elasticity (see Equation 4). When considering the current experimental data, it was found that the function

proposed by Kaushik et al. (2007a) generally matched the field extracted and laboratory constructed sample test results, except that one of the equation constants, a, required adjustment to 0.21.

$$\varepsilon'_m = \frac{0.21 f'_m}{{f'_j}^{0.25} {E_m}^{0.7}} \quad (6)$$

Figure 6 illustrates the masonry strain at peak stress predicted using Equation 6 (using the experimental mean f'_m, f'_j and E_m) plotted against the experimentally determined mean masonry strain at peak stress, showing satisfactory agreement with R^2 = 74%.

Numerical modelling of masonry compression stress-strain behaviour

A numerical model for masonry compression stress-strain response that aligned with the current experimental data was proposed as an aid for structural engineers when performing non-linear structural analysis. The current experimental data was analysed by plotting all experimental stress-strain curves from each prism group for comparison with previously developed numerical models. It is noted that the grouted masonry damage parameter incorporated in the Seible and Kingsley (1991) model was not considered as the current experimental programme exclusively addressed solid clay brick masonry. The input parameters used for the proposed models were the experimental mean f'_m and ε'_m values. Figure 7 illustrates examples of the comparison plots for different field extracted and laboratory constructed prism combinations.

Figure 7 shows that in general, the Kaushik et al. (2007a) and the modified Seible and Kingsley (1991) models could be used to represent the average of the masonry stress-strain curves until peak stress was reached. However, the model suggested by Priestley and Elder (1983) did not satisfactorily match the current experimental data as at a given value of strain, this model predicted significantly higher stress values than were measured during testing. It is also noted

that the Priestley and Elder (1983) model could not predict the falling branch of the stress-strain curve when f'_m was lower than 6.9 MPa. Therefore, the post-peak masonry stress-strain curve was assumed as a horizontal plateau at peak stress when f'_m was lower than 6.9 MPa (refer to Figure 7(a),(b) and (d)).

When the damage parameter in the Seible and Kingsley (1991) model is excluded, the Seible and Kingsley (1991) model for $\varepsilon_m \leq 1.6\varepsilon'_m$ can be represented using Equation 3. Therefore, the Kaushik et al. (2007a) and the modified Seible and Kingsley (1991) models predicted identical stress-strain relationships until peak stress was reached. Their post-peak stress-strain branches descending to $0.9f'_m$ were also identical, with predicted response over this strain range aligning well with the current experimental data. Beyond $0.9f'_m$, the Kaushik et al. (2007a) model split into two different descending linear relationships depending on the type of mortar used, whilst the modified Seible and Kingsley (1991) model remains parabolic until $1.6\varepsilon'_m$.

It was assumed that the mortar compressive stiffness is related to the mortar compressive strength (as also found by Kaushik et al. (2007a)). Therefore, the mortar compressive strength was used as a measure to categorise the compression stress-strain behaviour of the field extracted and laboratory constructed prisms, regardless of their mortar composition and age. For prisms that were constructed using mortars having mean f'_j of 5 MPa and above (see Figure 7(e) and (f) for examples), their post-peak compression stress-strain curves could be predicted adequately using the Kaushik et al. (2007a) model for prisms constructed using cement-lime mortars (referred to as "Kaushik et al. (CL)" in Figure 7).

Prisms that were constructed using mortars having mean f'_j below 5 MPa (see Figure 7(a) to (d) for examples) had lower post-failure strains than those constructed using mortars having mean $f'_j \geq 5$ MPa, and were best represented using the Kaushik et al. (2007a) model for prisms

constructed using cement mortar (referred to as "Kaushik et al. (C)" in Figure 7). Despite being similar, the Kaushik et al. (2007a) (C) model was preferred to the modified Seible and Kingsley (1991) model because of its simpler form.

In agreement with Kaushik et al. (2007a), the stress-strain behaviour of prisms that were constructed using cement rich cement-lime mortar (volumetric ratio of cement/lime ≥ 1.0) were best represented using the Kaushik et al. (2007a) (CL) model. However, the stress-strain response of prisms that were constructed using lime rich cement-lime mortars (volumetric ratio of cement/lime < 1.0) and of prisms that were constructed using pure lime mortar matched the Kaushik et al. (2007a) (C) model, which was intended for prisms constructed using pure cement mortar. This similarity was due to the dominance of lime in the mortar. Although the addition of lime into cement mortar increases ductility (Kaushik et al. 2007a), it was identified that the high lime proportion in the mortar resulted in weak and soft mortar joints which became completely crushed immediately after the peak stress was reached, thus provided little ductility to the masonry.

It is noted that a large proportion of the experimental stress-strain data was only recorded up to strains corresponding to $0.5f'_m$ on the descending branch (as shown in Figure 7) as it was difficult to record accurate stress and strain values beyond that point. However, the experimental results adequately matched the Kaushik et al. (2007a) model for the descending branch prior to $0.5f'_m$, and therefore the models proposed by Kaushik et al. (2007a) were selected for adoption.

SUMMARY AND CONCLUSIONS

The compressive strength and the Modulus of Elasticity were determined for 120 masonry prisms that were either extracted from eight New Zealand URM buildings or were constructed in

373 the laboratory using 14 different brick/mortar combinations. Experimental results were used to
374 develop predictive expressions and numerical models for the compressive behaviour of clay
375 brick masonry, using only the brick unit and mortar compressive strengths, to assist structural
376 engineers when undertaking detailed analysis. The following conclusions were drawn based on
377 the experimental results:
378 The brick unit and mortar properties, masonry compressive strength, Modulus of Elasticity and
379 strain at peak stress of the laboratory constructed samples generally aligned well with those of
380 the field extracted samples. The mean masonry compressive strength was found to increase with
381 increasing mean brick unit and mean mortar compressive strengths. A predictive equation
382 relating f'_b, f'_j and f'_m in the form of the Eurocode 6 expression (CEN 2005) was derived, and
383 constants K, α and β were found to be 0.75, 0.75 and 0.31 using the mean material compressive
384 strengths.
385 When the data sets for the field extracted and the laboratory constructed sample test results were
386 combined, the masonry Modulus of Elasticity was satisfactorily equated to $294f'_m$. One reason
387 for the derived constant (k) value being lower than is customarily recommended was that the
388 masonry Modulus of Elasticity was calculated using the stress and strain ordinates at $0.05f'_m$ and
389 $0.70f'_m$ instead of those located at $0.05f'_m$ and $0.33f'_m$ as used by previous researchers. This
390 adopted calculation method generated stiffness values appropriately reflecting the non-linear
391 behaviour for the strain range up to ε'_m, and therefore although the derived E_m values were low,
392 they were thought to be more representative for use in linear and non-linear seismic analyses.
393 The predictive expression proposed by Kaushik et al. (2007a) to estimate masonry strain at peak
394 stress generally matched the field extracted and laboratory constructed sample test results, except
395 that one of the equation constants, a, required adjustment from 0.27 to 0.21.

For the masonry compression stress-strain numerical model, it was found that the Kaushik et al. (2007a) (CL) model was suitable for prisms that were constructed using mortars having mean $f'_j \geq 5$ MPa, whilst prisms that were constructed using mortars having mean $f'_j < 5$ MPa could be represented by the Kaushik et al. (2007a) (C) model.

It was theorised that the post-peak stress-strain behaviour of prisms that were constructed using lime rich cement-lime mortar and using pure lime mortar was similar to the Kaushik et al. (2007a) (C) model due to the dominance of lime in the mortar used in this experimental programme. This dominance resulted in weak and soft mortar joints that crushed immediately after their peak strength was reached, thus providing little ductility to the masonry.

REFERENCES

Aryana, S. A., and Matthys, J. H. (2008). "Statistical Analysis of Compressive Strength of Clay Brick Masonry: Testing." *The Masonry Society Journal*, 26(2), 43-51.

ASTM (1997). "Standard Test Method for Young's Modulus, Tangent Modulus, and Chord Modulus." *E 111 - 97*, ASTM International, Pennsylvania, United States.

ASTM (2003a). "Standard Test Method for Compressive Strength of Masonry Prisms." *C 1314 - 03b*, ASTM International, Pennsylvania, United States.

ASTM (2003b). "Standard Test Methods for Sampling and Testing Brick and Structural Clay Tile." *C 67 - 03a*, ASTM International, Pennsylvania, United States.

ASTM (2008a). "Standard Specification for Mortar for Unit Masonry." *C 270 - 08a*, ASTM International, Pennsylvania, United States.

ASTM (2008b). "Standard Test Method for Compressive Strength of Hydraulic Cement Mortars (Using 2-in. or [50-mm] Cube Specimens)." *C 109/C 109M - 08*, ASTM International, Pennsylvania, United States.

CEN (2005). "Eurocode 6: Design of masonry structures - Part 1-1: General rules for reinforced and unreinforced masonry structures." *EN 1996-1-1:2005*, European Committee for Standardization, Brussels, Belgium.

CSA (2004). "Design of Masonry Structures, S304.1." Canadian Standards Association, Ontario, Canada.

Deodhar, S. V. (2000). "Strength of Brick Masonry Prisms in Compression." *Journal of the Institution of Engineers (India)*, 81(3), 133-137.

Drysdale, R., Hamid, A., and Baker, L. (1999). *Masonry Structures: Behaviour and Design*, The Masonry Society, Boulder, Colorado, United States.

FEMA (1999). "Evaluation of earthquake damaged concrete and masonry wall buildings, basic procedures manual, ATC-43." *FEMA 306*, Federal Emergency Management Agency, California, United States.

Gumaste, K. S., Nanjunda Rao, K. S., Venkatarama Reddy, B. V., and Jagadish, K. S. (2006). "Strength and elasticity of brick masonry prisms and wallettes under compression." *Materials and Structures*, 40(2), 241-253.

Hendry, A. W. (1998). *Structural Masonry*, Macmillan Press, London, United Kingdom.

Kaushik, H. B., Rai, D. C., and Jain, S. K. (2007a). "Stress-Strain Characteristics of Clay Brick Masonry under Uniaxial Compression." *Journal of Materials in Civil Engineering*, 19(9), 728-738.

Kaushik, H. B., Rai, D. C., and Jain, S. K. (2007b). "Uniaxial compressive stress-strain model for clay brick masonry." *Current Science*, 92(4), 497-501.

Kent, D. C., and Park, R. (1971). "Flexural Members with Confined Concrete." *Journal of the Structural Division, ASCE*, 97(ST7), 1969-1990.

Kingsley, G. R., Noland, J. L., and Schuller, M. P. (1992). "The Effect of Slenderness and End Restraint on the Behavior of Masonry Prisms - A Literature Review." *The Masonry Society Journal*, 10(2), 31-47.

Lenczner, D. (1972). *Elements of load bearing brickwork*, Pergamon Press, Oxford, United Kingdom.

Lumantarna, R. (2012). "Material Characterisation of New Zealand Unreinforced Masonry Buildings." Doctor of Philosophy, The University of Auckland, Auckland, New Zealand.

Marcari, G., Manfredi, G., Prota, A., and Pecce, M. (2007). "In-plane shear performance of masonry panels strengthened with FRP." *Composites: Part B*, 38(7-8), 887-901.

Morel, J. C., Pkla, A., and Walker, P. (2007). "Compressive strength testing of compressed earth blocks." *Construction and Building Materials*, 21(2), 303-309.

MSJC (2002). "Building code requirements for masonry structures, ACI 530-02/ASCE 5-02/TMS 402-02." America Concrete Institute, Structural Engineering Institute of the American Society of Civil Engineers, The Masonry Society, Detroit, Michigan, United States.

NZSEE (2006). "Assessment and improvement of the structural performance of buildings in earthquakes." New Zealand Society for Earthquake Engineering, Wellington, New Zealand.

Oakdale Engineering (2010). "DataFit 9.0." Oakdale Engineering, Oakdale, United States. http://www.oakdaleengr.com/.

OPCM (2005). "Masonry Section of Annexe 2: Buildings of Ordinance PCM 3274 & Modifications OPCM 3431." Department of Civil Protection, Rome, Italy.

Paulay, T., and Priestley, M. J. N. (1992). *Seismic design of reinforced concrete and masonry buildings*, John Wiley & Sons, New York, United States.

Priestley, M. J. N., and Elder, D. M. (1983). "Stress-strain curves for unconfined and confined concrete masonry." *American Concrete Institute Journal*, 80(3), 192-201.

Russell, A., and Ingham, J. (2010). "Prevalence of New Zealand's Unreinforced Masonry Buildings." *Bulletin of The New Zealand Society for Earthquake Engineering*, 43(3), 182-201.

Sarangapani, G., Venkatarama Reddy, B. V., and Jagadish, K. S. (2005). "Brick-Mortar Bond and Masonry Compressive Strength." *Journal of Materials in Civil Engineering*, 17(2), 229-237.

Seible, F., and Kingsley, G. R. (1991). "Modeling of Concrete and Masonry Structures subjected to Seismic Loading." *Experimental and numerical methods in earthquake engineering*, J. Donéa, ed., Kluwer Academic Publishers, Dordrecht, The Netherlands, 281-318.

TABLES

Table 1: Field extracted sample constituent material properties

Field Site	City of Origin	Year of Construction	Mean f'_b MPa *(CoV)*	n	Mean f'_j MPa *(CoV)*	n
AH	Wellington	1884	8.5 *(0.18)*	17	1.23 *(0.17)*	7
BC	Auckland	1886	12.0 *(0.28)*	14	4.54 *(0.13)*	6
AL	Gisborne	1906	15.7 *(0.21)*	20	5.53 *(0.14)*	8
CFK	Auckland	1910	16.0 *(0.11)*	10	4.14 *(0.18)*	14
HC	Wellington	1881	16.3 *(0.20)*	8	8.58 *(0.16)*	16
D	Auckland	1940s	17.1 *(0.15)*	7	2.62 *(0.19)*	16
TA	Te Awamutu	1946	21.1 *(0.23)*	9	5.92 *(0.17)*	8
RB	Auckland	1930s	27.3 *(0.21)*	32	6.65 *(0.21)*	11

Table 2: Laboratory constructed sample constituent material properties

Brick Group	Mean f'_b MPa *(CoV)*	n	Mortar Grade	Proportion by Volume				Equivalent classification	Mean f'_j MPa *(CoV)*	n
				Cement	Lime	Sand	Water			
AH	8.5 *(0.18)*	17	A	0	1	3	2.8	NZSEE 'firm'	0.69 *(0.13)*	5
SB	10.6 *(0.25)*	13	B	0	2	3	n.a*	Mason**	1.75 *(0.08)*	5
AL	15.7 *(0.21)*	20	C	1	3	12	3.4	ASTM 'K'	2.47 *(0.04)*	5
D	17.1 *(0.15)*	7	D	1	2	9	2.1	ASTM 'O'	4.95 *(0.14)*	5
RB	27.3 *(0.21)*	32	E	1	1	9	n.a*	Mason**	5.90 *(0.11)*	5
NL	27.5 (0.22)	19	F	1	1	6	1.3	ASTM 'N'	8.65 *(0.04)*	5
HB	38.6 *(0.16)*	21	G	1	1	6	n.a*	ASTM 'N'	12.52 *(0.26)*	5
ST	43.4 *(0.15)*	9	H	4	1	12	4	NZSEE 'stiff'	23.20 *(0.09)*	5

* - Water : cement ratio was kept constant, but was not recorded

** - Mix approximated by mason assisting in the sample construction process

514 Table 3: Field extracted and laboratory constructed prism properties

Prism Group	Mean f'_b MPa	Mean f'_j MPa	Mean f'_m MPa *(CoV)*	n	Mean f'_m* MPa *(CoV)*	n*	Mean E_m MPa *(CoV)*	Mean ε'_m MPa *(CoV)*	Mean E_m/f'_m
Field									
AH	8.5	1.23	3.31 *(0.19)*	5	3.32 *(0.22)*	4	388 *(0.30)*	0.0105 *(0.21)*	118
BC	12.0	4.54	6.98 *(0.25)*	6	7.59 *(0.22)*	5	2,252 *(0.31)*	0.0048 *(0.21)*	296
AL	15.7	5.53	10.70 *(0.09)*	6	10.88 *(0.08)*	4	2,133 *(0.16)*	0.0079 *(0.14)*	197
CFK	16.0	4.14	7.39 *(0.12)*	6	7.76 *(0.09)*	4	1,861 *(0.25)*	0.0061 *(0.32)*	241
HC	16.3	8.58	6.59 *(0.23)*	6	6.86 *(0.23)*	5	1,963 *(0.35)*	0.0051 *(0.39)*	285
D	17.1	2.62	6.06 *(0.15)*	4	6.06 *(0.15)*	4	1,492 *(0.26)*	0.0073 *(0.33)*	256
TA	21.1	5.92	12.05 *(0.12)*	6	12.75 *(0.03)*	6	4,004 *(0.11)*	0.0044 *(0.11)*	314
RB	27.3	6.65	14.70 *(0.21)*	6	15.11 *(0.11)*	5	4,286 *(0.24)*	0.0049 *(0.30)*	283
Lab									
AH-D	8.5	4.95	6.19 *(0.18)*	5	6.51 *(0.15)*	4	899 *(0.20)*	0.0099 *(0.07)*	138
SB-B	10.6	1.75	7.17 *(0.14)*	5	7.34 *(0.14)*	4	644 *(0.11)*	0.0143 *(0.17)*	89
SB-G	10.6	12.52	9.35 *(0.22)*	5	9.35 *(0.22)*	5	1,474 *(0.43)*	0.0089 *(0.34)*	155
AL-D	15.7	4.95	10.82 *(0.13)*	6	11.19 *(0.12)*	4	3,047 *(0.17)*	0.0048 *(0.14)*	274
AL-H	15.7	23.20	16.78 *(0.19)*	6	15.90 *(0.18)*	4	5,692 *(0.21)*	0.0030 *(0.20)*	357
D-A	17.1	0.69	7.35 *(0.25)*	7	7.19 *(0.17)*	6	926 *(0.28)*	0.0095 *(0.23)*	132
D-C	17.1	2.47	10.63 *(0.10)*	6	10.18 *(0.09)*	5	2,851 *(0.32)*	0.0050 *(0.24)*	279
D-D	17.1	4.95	11.71 *(0.08)*	4	11.71 *(0.08)*	4	4,295 *(0.13)*	0.0033 *(0.11)*	366
D-E	17.1	5.90	11.52 *(0.15)*	4	11.52 *(0.15)*	4	3,904 *(0.14)*	0.0032 *(0.17)*	342
D-F	17.1	8.65	16.07 *(0.18)*	7	16.24 *(0.19)*	6	6,019 *(0.23)*	0.0036 *(0.11)*	371
D-H	17.1	23.20	16.68 *(0.13)*	5	16.68 *(0.13)*	5	7,227 *(0.25)*	0.0028 *(0.18)*	433
NL-D	27.5	4.95	14.66 *(0.13)*	6	12.94 *(0.17)*	5	3,319 *(0.33)*	0.0067 *(0.32)*	253
HB-G	38.2	12.52	30.79 *(0.13)*	5	30.79 *(0.13)*	5	7,971 *(0.30)*	0.0050 *(0.25)*	257
ST-G	43.4	12.52	24.77 *(0.14)*	4	24.77 *(0.14)*	4	7,189 *(0.39)*	0.0047 *(0.18)*	285

515

516

Figure
Click here to download Figure: Figure 1.pdf

Figure 1: Preparation of field extracted prisms

Figure
Click here to download Figure: Figure 2.pdf

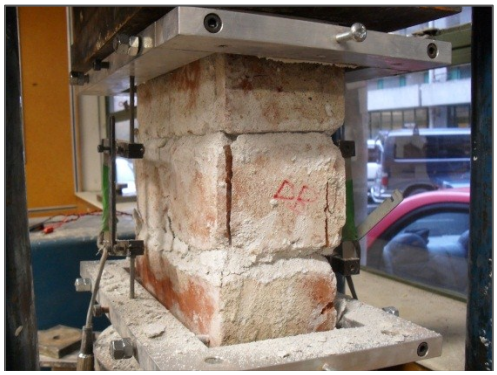

Figure 2: Prism compression test

Figure
Click here to download Figure: Figure 3.pdf

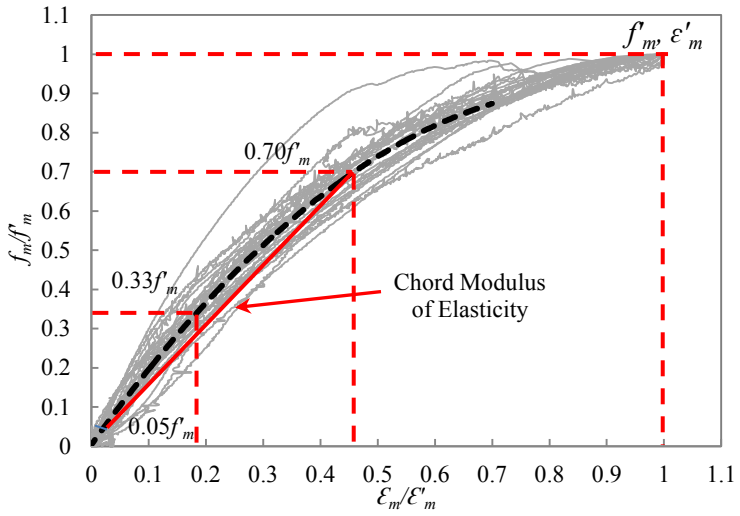

Figure 3: Masonry prism compression stress-strain curve, showing interpretation of E_m

Figure
Click here to download Figure: Figure 4.pdf

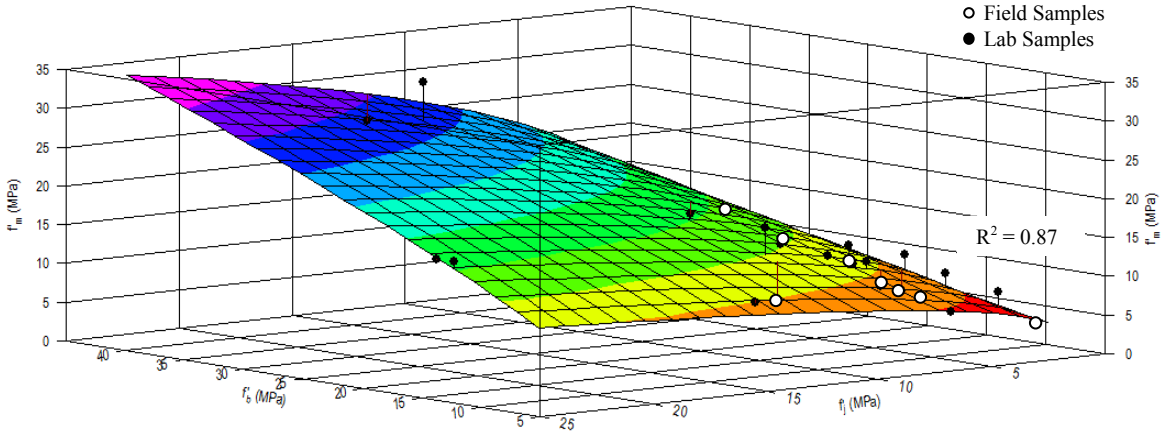

Figure 4: Three-dimensional plot relating f'_b, f'_j and f'_m

Figure
Click here to download Figure: Figure 5.pdf

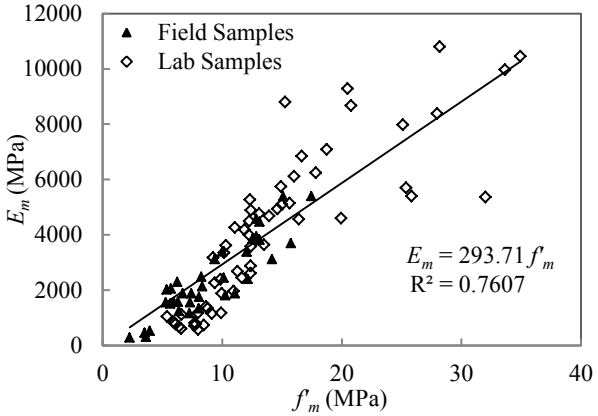

Figure 5: The E_m-f'_m relationship of both field extracted and laboratory constructed samples

Figure
Click here to download Figure: Figure 6.pdf

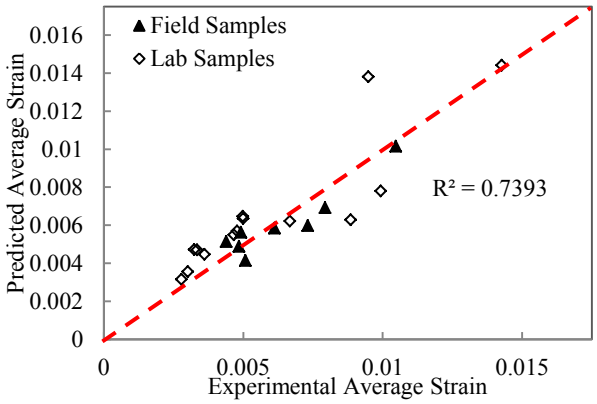

Figure 6: Comparison between predicted vs. experimental strain at peak stress

Figure
Click here to download Figure: Figure 7.pdf

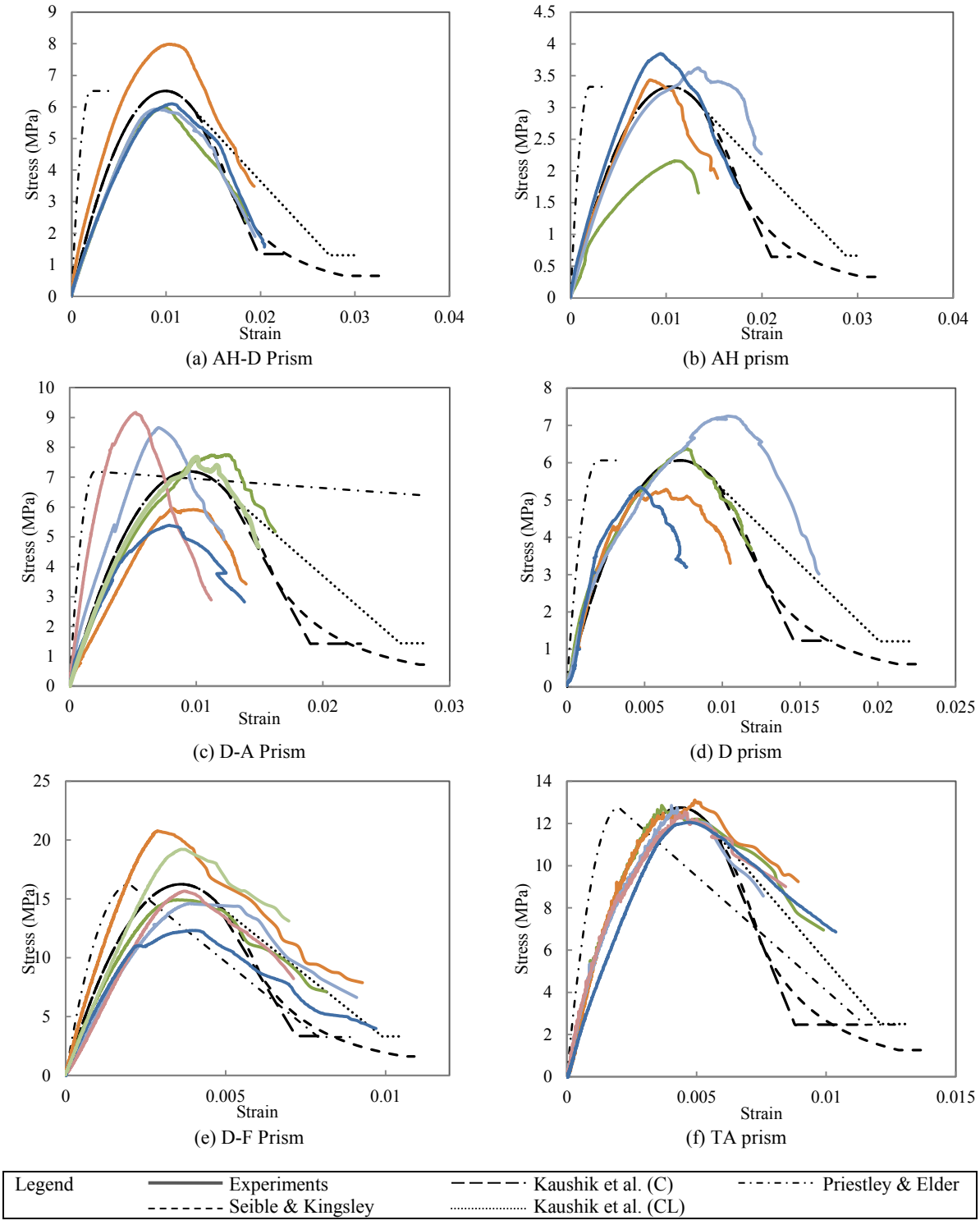

Figure 7: Comparison between experimental and numerical stress-strain curves

LIST OF FIGURES